

# Periodicities in Aerosol Optical Depths

S. Ramachandran<sup>1</sup>, Sayantan Ghosh<sup>2</sup>, Prasanta K. Panigrahi<sup>3</sup> and Amit Verma,<sup>4</sup>

---

<sup>1</sup>Physical Research Laboratory,

Navrangpura, Ahmedabad 380009, India.

<sup>2</sup>School of Physics, University of

KwaZulu-Natal, Durban 4000, South Africa.

<sup>3</sup>Indian Institute of Science Education

and Research, Kolkata 741252, India.

<sup>4</sup>Department of Computer and

Information Science and Engineering,

University of Florida, Gainesville, Florida

32611, USA.

We investigate the temporal and spatial variability in aerosol optical depth (AOD) over different geographic locations in India due to their important role in the earth-atmosphere radiation budget. The use of continuous wavelet transform pinpoints the spatio-temporal non-stationarity of the periodic variations in the AOD depending on local factors. The optimal time-frequency localization ability of Morlet wavelet accurately isolates the periodic features in the different frequency domains, to study the variations in the dominant periods due to local effects. The origin of the effects on the periodic modulations is then related to physical phenomena of regional nature, which throws considerable light on the observed variations in aerosol optical depths. We also find the phase relationship between different locations and to identify the possible correlations between different geographic locations and related environmental variations.

## 1. Introduction

Atmospheric aerosols influence the earth's climate in many important ways. Aerosols interact directly and indirectly with solar radiation and give rise to radiative forcing. The direct interaction of aerosols involves both scattering and absorption of radiation, while the indirect effect of aerosols on climate occurs by modifying the optical properties and lifetimes of clouds. Aerosol radiative forcing remain a significant uncertainty for climate studies (see for e.g. *Houghton et al.* [2001]; *Solomon et al.* [2007]). The sources of aerosols are widely varied and differ on a regional basis leading to regional variations on the earth's radiative budget (see for e.g. *Houghton et al.* [2001]; *Solomon et al.* [2007]; *Ramanathan et al.* [2001]; *Bellouin et al.* [2005]). Expectedly, the physical and chemical properties of aerosols are strong functions of their sources. The spatial and temporal variabilities in aerosols are of significant interest for modeling their climate impact. However, global observations of columnar aerosol features have only been possible from the satellite payloads during the last five to six years, e.g., Polarization and Directionality of Earth's Reflectances (POLDER), Multi-angle Imaging Spectroradiometer (MISR) and Moderate Resolution Imaging Spectroradiometer (MODIS), onboard Terra and Aqua satellites. The paucity of sufficient data necessitates the use of sophisticated analysis techniques for extracting meaningful behavior in aerosol characteristics. In particular, any meaningful structured variations like cyclic or periodic ones are of deep interest, both for their physical origin, as well as for climate modeling. The populated tropical regions have been found to contribute the most to the global aerosol surface forcing, with Asia being the largest contributor (see for e.g. *Ramanathan et al.* [2001]). Asia accounts for

about 60% of the world's population of 6000 million. India is densely populated, industrialized and in the recent years has witnessed impressive economic development. The growing population and globalization coupled with revolution in industry has resulted in higher demands for energy, transport and communications (see for e.g. *Chung et al.* [2005]). Indian subcontinent, apart from being a source region for aerosols, is bordered by densely populated and industrialized areas on the east and western sides, from where different aerosol species, such as mineral dust, soot, nitrates, sulfate particles and organics are produced and transported, thus making it a regional aerosol hot spot. The Indian landmass covers coastal regions, inland plains, semi-arid regions, mountains and plateau regions. This subcontinent experiences tropical and subtropical climatic conditions, resulting in extreme temperatures, rainfall and relative humidity. These features introduce large variabilities in aerosol characteristics on spatial and temporal scales over India.

Recently, the interannual and seasonal variations in aerosol characteristics across India have been studied (see for e.g. *Chung et al.* [2005]; *Remer et al.* [2005]). The study was undertaken by dividing India into seven regions based on geography and meteorology, within the context of urban and rural development patterns, where Moderate Resolution Imaging Spectroradiometer (MODIS) Level 3 collection V005 aerosol products at  $1^\circ \times 1^\circ$  grid resolution (see for e.g. *Ramachandran and Cherian* [2008]) were used. The expected errors in MODIS aerosol optical depths (AOD) are  $\Delta\text{AOD} = \pm 0.03 \pm 0.05\text{AOD}$  over oceanic regions and  $\Delta\text{AOD} = \pm 0.05 \pm 0.15\text{AOD}$  over land (see for e.g. *Chung et al.* [2005]). These AODs have been validated with collocated Aerosol Robotic Network (AERONET) inversions at island and coastal sites (see for e.g. *Chung et al.* [2005]). It was found that

one standard deviation of MODIS effective radius retrievals falls within  $\Delta r_{eff} = \pm 0.11 \mu m$  (see for e.g. *Chung et al.* [2005]). Over India MODIS retrieved AODs have been validated with collocated AERONET AODs at Kanpur (26.4°N, 80.3° E) for the period January 2001-December 2005 (see for e.g. *Ramachandran* [2007]). AODs derived from MODIS and AERONET were found to compare well during January-May and August-December (see for e.g. *Ramachandran* [2007]). Aerosol optical depth at a particular location is dependent on a number of factors including the aerosol burden throughout the atmospheric column, the aerosol size distribution, and the chemical composition (as it relates to water uptake and refractive index). AODs can exhibit periodic or cyclic variations depending on natural and man made sources over a region, which can get modulated by the meteorological conditions such as winds, rainfall and relative humidity. Transport of dust and sea salt from the adjacent source regions can also modulate the periodic nature of AODs (see for e.g. *Prospero et al.* [2002]; *Kaufman et al.* [2002]). Daily mean MODIS AOD data were averaged to obtain the monthly mean AOD over 35 locations which are the capitals of the states and union territories in India (see for e.g. *Kaufman et al.* [2002]). Monthly averaged data for 96 months (January 2001-December 2008) are analyzed here to determine the periodicities in AODs over various regions in India, in order to ascertain the extent and nature of local variations.

Wavelet transform has recently emerged as a powerful tool to study the transient and time varying phenomena (see for e.g. *Daubechies* [1992]; *Mallat* [1999]). It is an ideal tool for identifying variations at multiple scales. In particular, continuous Morlet wavelet has optimal sensitivity making it a good choice for observation of long term periodicities. The

optimal sensitivity of wavelets to both high and low scale variations has already found application in the merger of different proxy data for establishing weather variations on the millennial scale (see for e.g. *Moberg et al.* [2005]).

This letter is organized as follows. In the Sec. 2, we have discussed the methodology and theory, where, we have briefly reviewed the wavelet transform and the phase relations obtained through them. Then we report our observations and discuss their implications and sources in Sec. 3 and we then we conclude with the inferences and impacts we draw from this work.

## 2. Methodology and theory

In this section we outline the Continuous Wavelet Transform (CWT) and explain the phase information obtained from the Complex Continuous Wavelet Transform. Wavelet Transform, since its advent has been a valuable tool for signal processing (see for e.g. *Daubechies* [1992]; *Torrence and Compo* [1998]). It has been applied to analyze signals from a myriad number of areas and has also been applied to study geophysical data like El Niño Southern Oscillations (see for e.g. *Torrence and Compo* [1998]), tropical convection over the western Pacific (see for e.g. *Weng and Lau* [1994]) amongst others. A detailed description of the use of wavelet transforms to Geophysics can be found in *Foufoula-Georgiou and Kumar* [1995]. The CWT of a data set  $X = \{x_i\}, i \in \mathbb{Z}^+$ , is given by,

$$W_i(s) = \sum_{j=1}^{N-1} x_j \psi^* \left( \frac{i-j}{s} \right) \quad (1)$$

where,  $s$  is the scale and  $N$  is the data length.  $\psi(s)$  is a well localized (in both physical and Fourier domains), zero mean and integrable function and is called the *mother wavelet*.

The Eq 1 represents a convolution equation, where the wavelet coefficients calculated by convolving the scaled and translated versions of  $\psi(n)$  with  $x_i$ . This makes it clear that  $s$  is the scaling parameter and  $j$  the translation parameter. In this analysis, we use the Morlet wavelet, given by,

$$\psi(n) = C \cos(5n) e^{-\frac{n^2}{2}} \quad (2)$$

where  $C$  is a normalization constant. This function has a wide support which allows us to get more accurate results from the computationally performed convolution. Since this function is real, we will use it to extract periodic structures from the AOD data, while in order to obtain the phase relationships between various stations, we will use the complex Morlet function given by,

$$\psi(n) = \frac{1}{\sqrt{\pi F_b}} \exp \left( 2i\pi F_c n - \frac{n^2}{F_b} \right) \quad (3)$$

where  $F_b = 1$  and  $F_c = 1.5$  are the bandwidth parameter and wavelet center frequencies respectively (see *Teolis* [1998]). The phase angle is given by,

$$\phi(n) = \tan^{-1} \left( \frac{\text{Im}[\psi(n)]}{\text{Re}[\psi(n)]} \right) \quad (4)$$

Since the data length is small, the analysis was limited to a scale of 32. As shown in Fig. 2, the cone of influence is not small enough to make the wavelet coefficients unusable at this scale.

### 3. Results and Discussion

As mentioned in the earlier section, the Continuous Wavelet Transform was used to analyze the AOD monthly averaged data of 35 stations in India. Subsequently the obtained

periodicities are also checked through Mexican hat wavelets. Results obtained over India  
 are broadly categorized into 4 groups due to their common characteristics. We observe  
 the presence of three dominant periods in the signal, one corresponding to 12 months  
 and the others corresponding to approximately 24 and 48 months. This is represented  
 in the Fig.1; which shows the monthly averaged AOD data and the local variation in  
 various geographical regions, obtained using Morlet wavelet technique for Chennai (south  
 India), Mumbai (west India), Bengaluru (south India) and Kohima (northeast India).  
 Though the 12 month period is a stationary period (i.e., it does not vary over time), the  
 24 months period is non stationary. We also observe a period of approximately 5 months  
 for all the locations. This is indicative of an external influence (over the natural cycle)  
 in the Aerosol Optical Depth for the locations observed. *Satheesh et al.* [2011] and *Sat-  
 tilingam Devara and Pal* [2004] have observed a weekly period of AOD over urban centers  
 like Bengaluru and Pune in India. In our case, we do not observe such modulations since  
 we have a monthly averaged data, rendering the smaller scale modulations invisible. The  
 Quasi-Biennial Oscillations are confirmed by the observations of *Beegum et al.* [2009] in  
 the spectral AOD data. We also observe an approximately 48 months cycle in the AOD  
 which appears only after sufficient averaging. This implies the presence of long term  
 correlations in the AOD over the locations at which the data was collected.

In Fig. 3, we plot the phase relations obtained using Eq. 4. These obtained phase  
 relations are very interesting in the sense that we observe a stationarity in the phases at  
 scale 20 (denoted by the blue plot). In contrast, at scale 10 (denoted by red), which is  
 the high frequency range, we observe non-stationarity in the phases. At scale 30 (denoted



by the black line), we observe that all the stations undergo a phase variation around the month 35. Though Chennai recovers the fastest, the other stations take a considerable time to recover to their original phases giving us a measure of their recovery time. The low frequency range is also non-stationary. This makes the analysis of their phase differences important. In Fig. 4; we depict the phase differences between the various stations. We observe that at scale 20 (mid frequency range), the stations are periodically in and out of phase, while Chennai stays in phase with Mumbai and Bengaluru most of the time. Also, Bengaluru and Mumbai stay in phase for some time. It should be noted here that  $\Delta\phi = 0$  means zero phase lag, while  $\Delta\phi > 0$  means the first station leads the phase and  $\Delta\phi < 0$  means the second station leads the phase. The observation about the recovery time in Fig. 3 is corroborated by the Fig. 4. As the individual phases take a long time to recover, the phase differences also correspondingly long time to recover. This long recovery time could correspond to an external modulation from the industrial activity around the locations.

AODs over Chennai, Bengaluru and Mumbai are found influenced by anthropogenic processes but the aerosol distribution gets modulated by natural sources such as sea salt and dust, while Kohima in the north-east at an altitude of 1.4 km ASL, is dominated by natural aerosols (see for e.g. *Ramachandran* [2007]; *Ramachandran and Cherian* [2008]). In northeast India because of the large forest cover aerosols from biomass burning and forest fires dominate the distribution, thus making it a natural aerosol source region (see for e.g. *Habib et al.* [2006]). The northeast region is less densely populated and so man made contribution to AODs will be minimal. A strong seasonal variation in AODs

(summer monsoon high) was seen in Mumbai and Chennai (see for e.g. *Ramachandran* [2007]).

An annual cycle in AODs over the urban locations arises due to the summer high and winter low in AODs. The increase in AODs during summer monsoon season is due to the prevailing strong convection in summer which results in a deeper boundary layer providing a longer atmospheric column for accommodating more of both natural and anthropogenic aerosols and hygroscopic growth of fine mode pollution (water soluble e.g., sulfate) aerosols at higher relative humidity (see for e.g. *Remer et al.* [2005]). In urban areas the local production of aerosols from anthropogenic activities such as fossil fuel combustion is not expected to significantly change during a year. The ratios of AOD between Jun-Sep (southwest, summer monsoon) and Jan-Mar (northeast, winter monsoon) is found to be higher than one in the four metro locations of Chennai, Mumbai, New Delhi and Kolkata (see for e.g. *Ramachandran and Cherian* [2008]). Higher than one AOD ratios over urban areas suggests seasonal variations in source strengths of natural aerosols, which coupled with hygroscopic growth of fine mode aerosols results in higher AODs during summer monsoon season.

#### 4. Conclusion

In conclusion, we have investigated the AOD over the 35 major urban centers of India through the Continuous Wavelet Transform in order to extract the periodic and local modulations present at various frequency ranges which are invisible to the conventional methods like Fourier Transform. We observed the presence of approximately 5 and 48 months periods in addition to the annual and Quasi-Biennial Oscillations. Also, in this

investigation, we pointed out the stability of the phases in the mid-frequency range, while in the high and the low frequency ranges, the phases are unstable implying time local disturbances in the high frequency range. The instability in the low frequency range could be attributed to long term changes in the atmospheric composition and structure over the locations due to various factors like industrial gases emission and change in forest cover. The interesting observation from this study is the phase relation between different locations, signifying that the modulations in one region affect the other. Since the 35 locations have been classified into four major regions, we can determine that the AOD variations in one region are affected by the other regions.

The investigation of AOD data over the Indian subcontinent through the CWT throws light on a number of things such as the presence of long term and short term modulations in the AOD, and also the correlated behavior of the AOD over various locations in a geographic neighborhood. This study could be furthered to investigate the nature of these fluctuations through more sophisticated wavelet based techniques to ascertain and correlate the various natural and man-made factors contributing to this behavior.

### Acknowledgments.

MODIS AOD data used in this study are downloaded using the NASA GES-DISC.

### References

- Beegum, S. N., K. K. Moorthy, S. S. Babu, R. R. Reddy, K. R. Gopal, and Y. N. Ahmed (2009), Quasi-biennial oscillations in spectral aerosol optical depth, *Atmospheric Science Letters*, 10(4), 279–284, doi:10.1002/asl.243.

- 178 Bellouin, N., O. Boucher, J. Haywood, and M. Reddy (2005), Global estimate of aerosol  
179 direct radiative forcing from satellite measurements, *Nature*, *438*, 1138–1141, doi:  
180 10.1038/nature04348.
- 181 Chung, C. E., V. Ramanathan, D. Kim, and I. A. Podgorny (2005), Global anthropogenic  
182 aerosol direct forcing derived from satellite and ground-based observations, *J. Geophys.*  
183 *Res.*, *110*, D24,207, doi:10.1029/2005JD006356.
- 184 Daubechies, I. (1992), *Ten lectures on wavelets*, 64 CBMS-NSF Regional Conference Series  
185 in Applied Mathematics, Society for Industrial Mathematics.
- 186 Foufoula-Georgiou, E., and P. Kumar (Eds.) (1995), *Wavelets in Geophysics*, 373 pp.,  
187 Academic Press.
- 188 Habib, G., C. Venkataraman, I. Chiapello, S. Ramachandran, O. Boucher, and  
189 M. Shekar Reddy (2006), Seasonal and interannual variability in absorbing aerosols  
190 over India derived from TOMS: Relationship to regional meteorology and emissions,  
191 *Atmos. Env.*, *40*(11), 1909–1921.
- 192 Houghton, J., et al. (Eds.) (2001), *IPCC 2001: Climate Change 2001: The Scientific Ba-*  
193 *sis. Contribution of Working Group I to the Third Assessment Report of the Intergov-*  
194 *ernmental Panel on Climate Change*, vol. 881, Cambridge University Press, Cambridge,  
195 United Kingdom and New York, NY, USA.
- 196 Kaufman, Y., D. Tanré, and O. Boucher (2002), A satellite view of aerosols in the climate  
197 system, *Nature*, *419*, 215–223, doi:10.1038/nature01091.
- 198 Mallat, S. (1999), *A Wavelet Tour of Signal Processing*, Academic Press.

- 199 Moberg, A., D. Sonechkin, K. Holmgren, N. Datsenko, and W. Karlen (2005), Highly  
200 variable Northern Hemisphere temperatures reconstructed from low- and high-resolution  
201 proxy data, *Nature*, *413*, 615–617, doi:10.1038/nature03265.
- 202 Prospero, J., P. Ginoux, O. Torres, S. Nicholson, and T. Gill (2002), Environmental  
203 characterization of global sources of atmospheric soil dust identified with the NIMBUS 7  
204 Total Ozone Mapping Spectrometer (TOMS) absorbing aerosol product, *Rev. Geophys.*,  
205 *40*, 1002–1033, doi:10.1029/2000RG000095.
- 206 Ramachandran, S. (2007), Aerosol optical depth and fine mode fraction variations deduced  
207 from moderate resolution imaging spectroradiometer (modis) over four urban areas in  
208 india, *J. Geophys. Res.*, *112*, D16,207, doi:10.1029/2007JD008500.
- 209 Ramachandran, S., and R. Cherian (2008), Regional and seasonal variations in aerosol  
210 optical characteristics and their frequency distributions over india during 2001-2005, *J.*  
211 *Geophys. Res.*, *113*, D08,207, doi:10.1029/2007JD008560.
- 212 Ramanathan, V., P. J. Crutzen, J. T. Kiehl, and D. Rosenfeld (2001), Aerosols, climate,  
213 and the hydrological cycle, *Science*, *294* (5549), 2119–2124, doi:10.1126/science.1064034.
- 214 Remer, L. A., et al. (2005), The modis aerosol algorithm, products and validation, *J.*  
215 *Atmos. Sci.*, *62*, 947–973.
- 216 Satheesh, S., V. Vinoj, and K. K. Moorthy (2011), Weekly periodicities of aerosol proper-  
217 ties observed at an urban location in india, *Atmospheric Research, In Press, Corrected*  
218 *Proof*, –, doi:DOI: 10.1016/j.atmosres.2011.03.003.
- 219 Sattilingam Devara, P. C., and S. Pal (2004), Wavelet Analysis of 14 Years’ Aerosol  
220 LIDAR Observations Over Pune India, in *22nd International Laser Radar Conference*

- 221 (*ILRC 2004*), *ESA Special Publication*, vol. 561, edited by G. Pappalardo & A. Amodeo,  
222 pp. 759–+.
- 223 Solomon, S., et al. (Eds.) (2007), *IPCC, 2007: Climate change 2007: The Physical Sci-*  
224 *ence Basis. Contribution of Working Group I to the Fourth Assessment Report of the*  
225 *Intergovernmental Panel on Climate Change*, New York: Cambridge University Press.
- 226 Teolis, A. (1998), *Computational signal processing with wavelets*, Birkhauser.
- 227 Torrence, C., and G. Compo (1998), A practical guide to wavelet analysis, *Bulletin of the*  
228 *American Meteorological Society*, 79(1), 61–78.
- 229 Weng, H., and K. M. Lau (1994), Wavelets, period doubling, and time-frequency local-  
230 ization with application to organization of convection over the tropical western Pacific,  
231 *Journal of Atmospheric Science*, 51, 2523–2541.

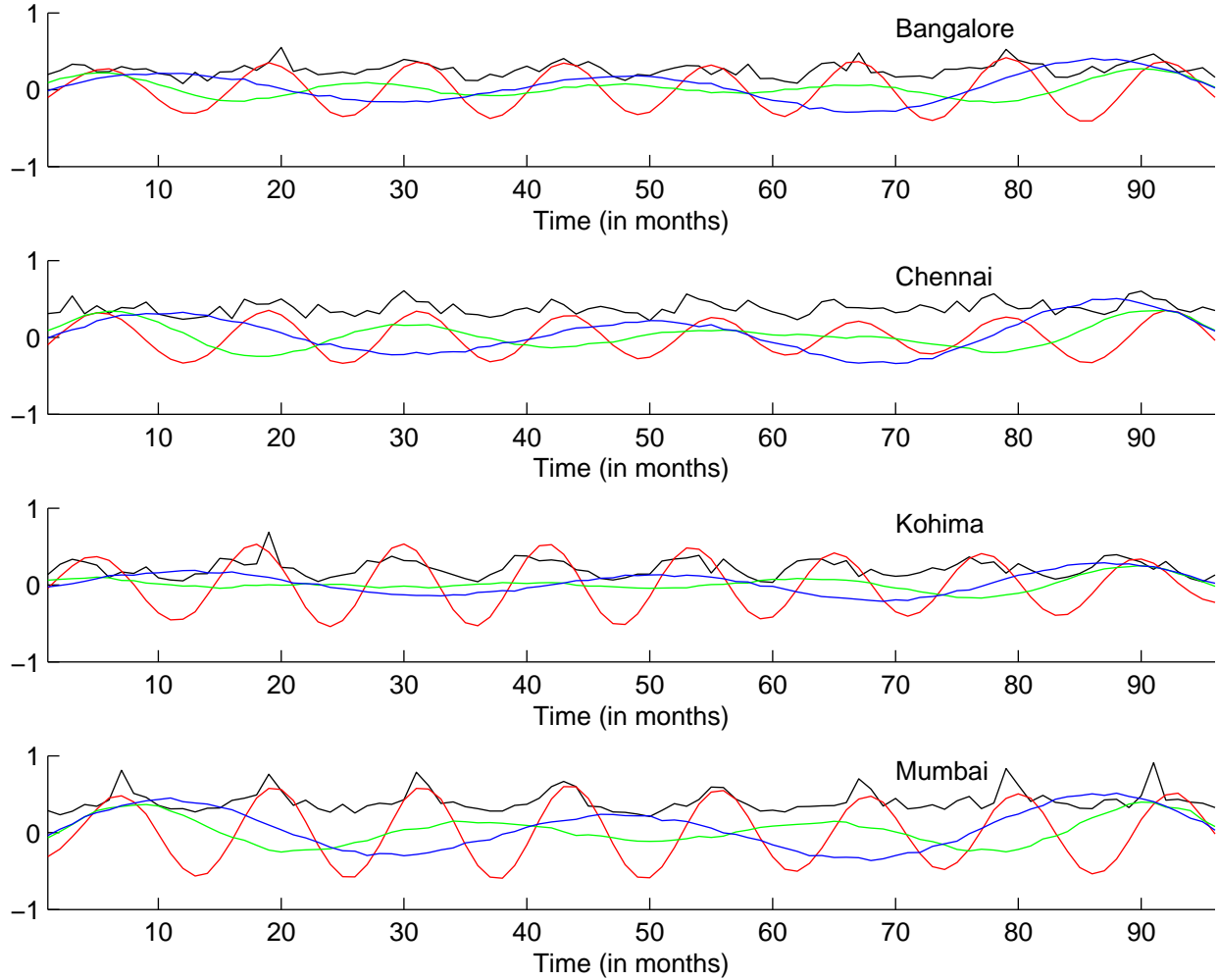


**Figure 1.** AOD data (black), superimposed with wavelet coefficients at scales 10 (red), 20 (green) and 30 (blue). The annual (red), QBO (green) and 40 (blue) month periods are clearly visible.

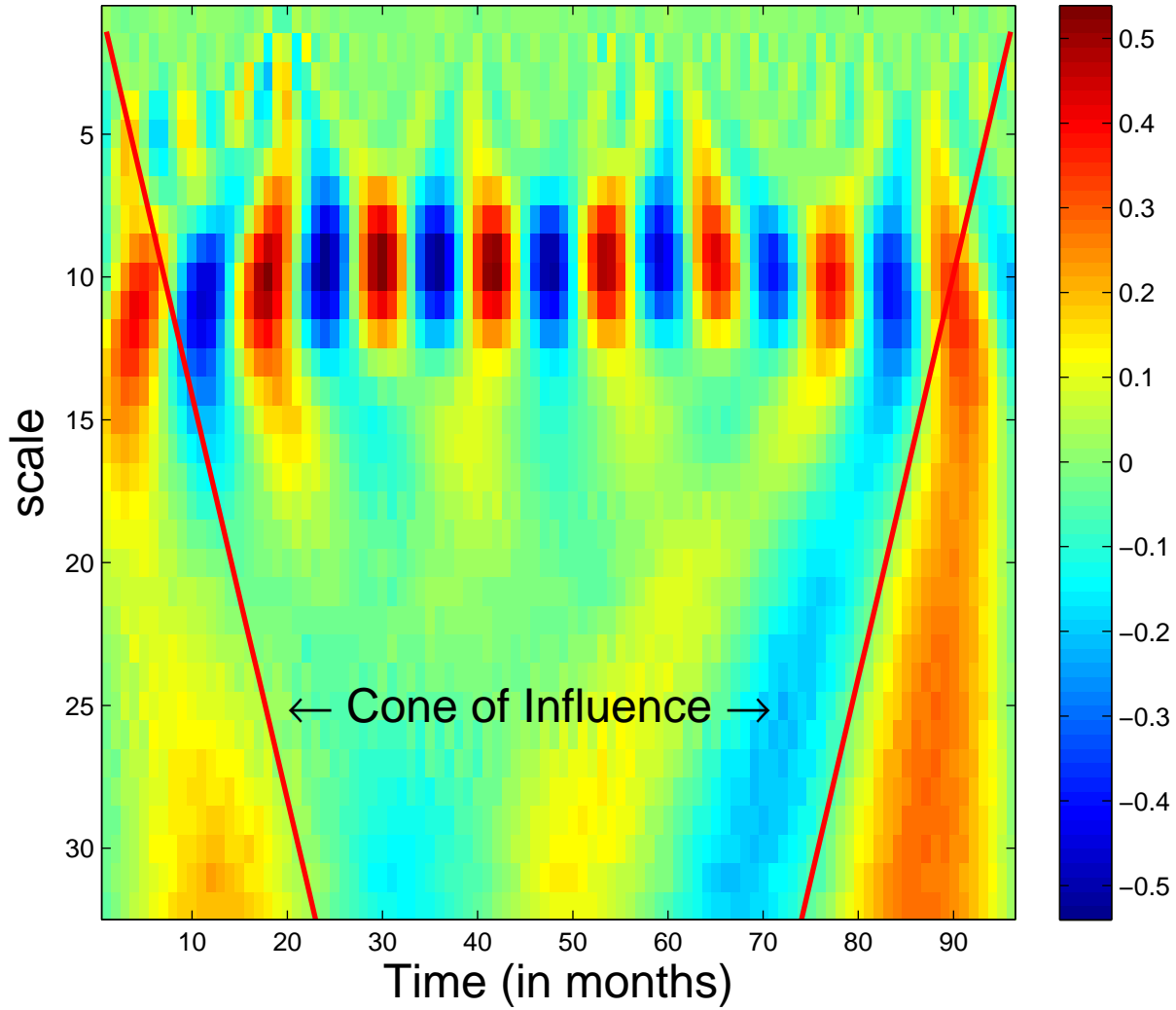


**Figure 2.** The scalogram for Kohima upto scale 32. The cone of influence is indicated. The annual (at scale 10), QBO (at scale 20) and 40 month (at scale 30) are clearly visible. The 5 month period is also visible at scale 5.



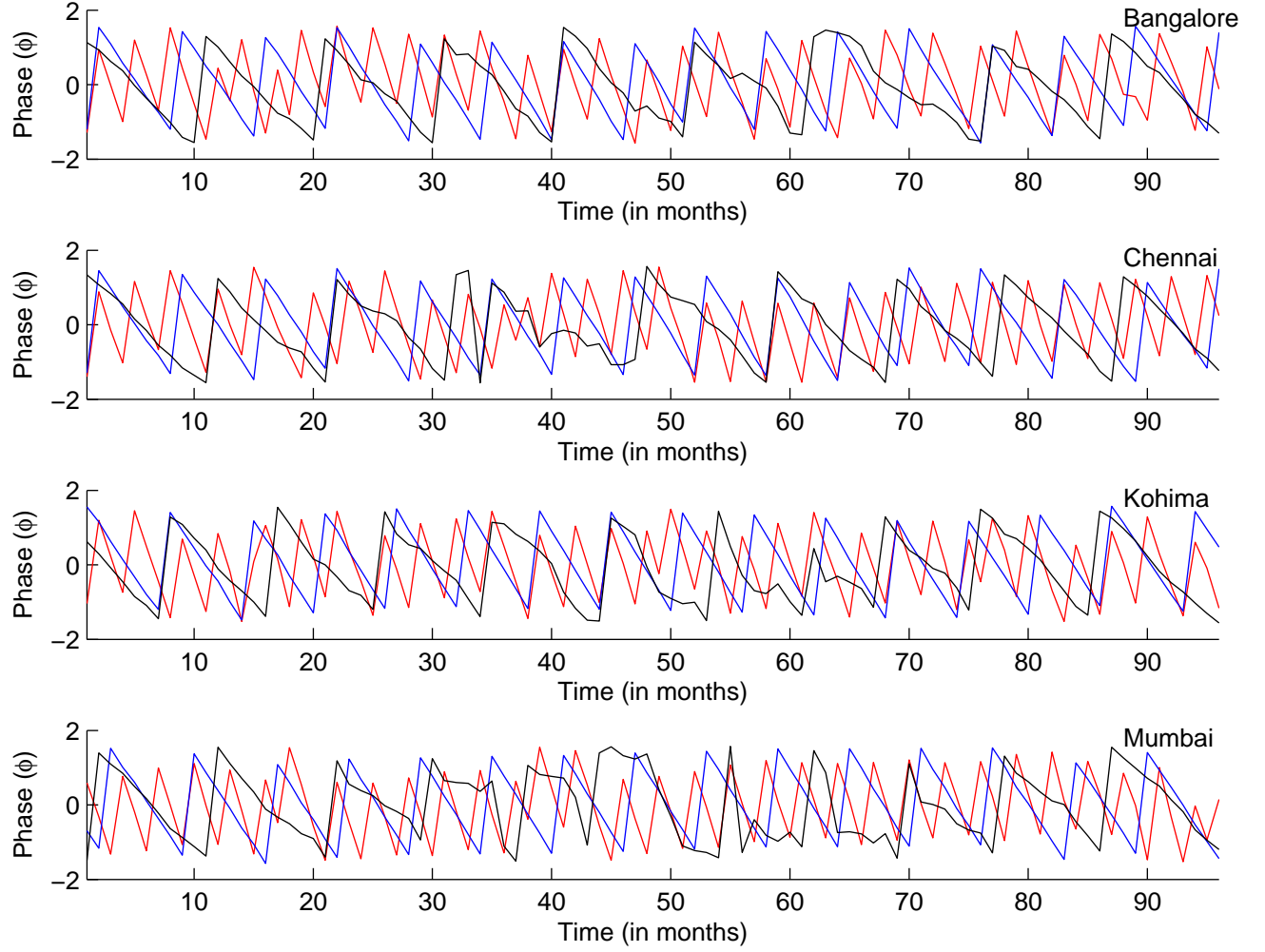


**Figure 3.** The phase relation at scale 10 (red), scale 20 (blue) and scale 30 (black) are shown. At scale 20, a stationary phase is seen, where as, at scales 10 and 30, the phases are non-stationary. Around the month 35, an extreme fluctuation in the phase at scale 20 corresponding to the QBO is observed.

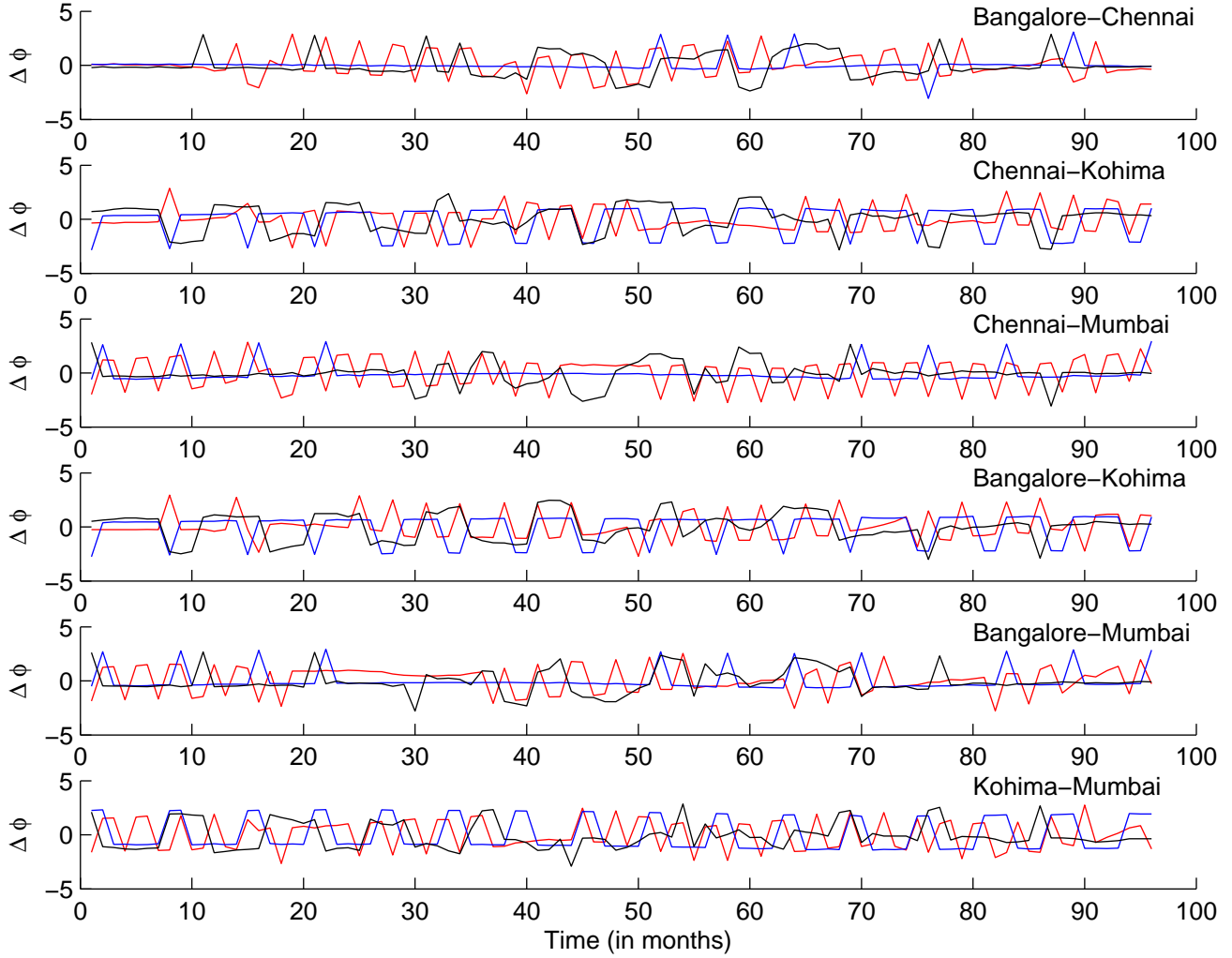


**Figure 4.** The phase differences between the four major locations at scale 10 (red), 20 (blue) and 30 (black). The positive phase difference  $\Delta\phi \equiv \phi_A - \phi_B > 0$  indicates that location  $A$  is leading location  $B$ , while  $\Delta\phi < 0$  indicates that location  $A$  is lagging behind location  $B$ .